MANA: Designing and Validating a User-Centered Mobility Analysis System

Boyd Anderson[1,2], **Shenggao Zhu**[1,2], **Ke Yang**[3], **Jian Wang**[3], **Hugh Anderson**[2], **Chao Xu Tay**[4],
Vincent Y. F. Tan[4,5], **Ye Wang**[1,2]
[1]School of Computing, National University of Singapore (NUS), Singapore
[2]NUS Graduate School for Integrative Sciences and Engineering, NUS, Singapore
[3]Huashan Hospital, Fudan University, Shanghai, China
[4]Department of Electrical and Computer Engineering, NUS, Singapore
[5]Department of Mathematics, NUS, Singapore
{boyd,shenggaozhu}@u.nus.edu, {yang_ke_1990,hs_wangjian336}@163.com, hugh@comp.nus.edu.sg,
taychaoxu@u.nus.edu, vtan@nus.edu.sg, wangye@comp.nus.edu.sg

ABSTRACT

In this paper, we demonstrate a new IMU-based wearable system (dubbed MANA or Mobility ANAlytics) for measuring gait in a clinical setting. The design process and choices that were made to ensure that the technology was invisible and accessible are described. We collect a rich and diverse dataset of walking data from sixty participants, including forty people with Parkinson's Disease (PD). The system is then validated in a clinical setting with this dataset. We present novel and innovative algorithms to measure common gait parameters. The system is able to estimate these gait parameters with high accuracy, with a mean absolute error of 4.0 cm for stride length and 2.6 cm for step length, outperforming all state-of-the-art methods that included data from people with PD.

Author Keywords

Mobility Analysis; Inertial Measurement Units; Wearable Sensors; User-centered design; Parkinson's Disease.

CCS Concepts

•**Applied computing** → *Life and medical sciences;* •**Human-centered computing** → *Accessibility;*

INTRODUCTION

The number of people aged 60 and over in the world is expected to more than double in the next forty years, from around 900 million people in 2015 to more than 2 billion in 2050 [26]. As a result, diseases that overwhelmingly affect older people such as stroke, osteoporosis (leading to osteoporotic fracture), and neurodegenerative disorders (e.g., Alzheimer's disease, Parkinson's Disease) will be a heightened economic and logistical challenge for society. The evaluation of these afflictions

involves a skilled medical professional, requires specialised equipment, and is both expensive as well as prone to human error. Therefore, inexpensive, scalable, accurate, objective, and, most importantly, accessible systems to help manage and diagnose such conditions are urgently needed.

A key consideration when designing any accessible or assistive technology is that there is often an implicit or explicit stigma associated with its use. It is important to take into account issues such as visibility of assistive technologies [10], customisability [33] and device aesthetics, device necessity and usage context [7], social acceptability, and age appropriateness, all common factors in creating a stigma that may lead to reducing the adoption of assistive technologies [29], to ensure that it is not only user-friendly but also that the stigmatisation of its users is kept to a minimum. To meet these requirements, we use a user-centred iterative design approach which considers the users needs at every stage of the design process [19]. In this process, understanding the user and their situation is of paramount importance [38].

In this study, our targeted users are people with Parkinson's Disease (PD). PD is a neurodegenerative disorder with no known cure. People with PD often have a decrease in the control of motor functions known as "parkinsonisms", such as bradykinesia (slowness of movement), rest tremors, rigidity, and postural and gait impairment. Due to the aforementioned aging population, its incidence is on the rise. Indeed, more than ten million people suffer from the condition[1].

Experiments have shown that even whilst on medication people with PD show a reduction in gait parameters such as cadence and stride length relative to age-matched healthy controls [28, 20]. In addition, people with PD attempting to perform motor tasks at a constant rate show larger variation than healthy controls performing the same tasks. For example, a study showed that people with PD have a larger step time variability (7%) than healthy controls (4%) [8]. Gait measurement in a clinical setting is normally quantified using pressure

---

[1]http://parkinson.org/Understanding-Parkinsons/Causes-and-Statistics/Statistics

sensitive walking mats [22], heel-mounted force-sensing sensors (or footswitches) [13], or motion-capture cameras [24]. All of these systems are costly, non-portable, often require either technical or clinical expertise to use, and as a result do not scale easily.

Additionally, medical specialists such as neurologists are a scarce resource in most countries, and smaller community hospitals in such countries are ill-equipped to make an accurate diagnosis of PD or even perform a mobility assessment, forcing (often frail) older people to travel a long distance to hospitals in large cities. To address this critical need, we demonstrate a cost effective and easily deployable Inertial Measurement Unit (IMU)-based system dubbed MANA (Mobility ANALytics) to ensure that long term mobility assessment becomes a reality for those with motor disabilities associated with PD. The system is low-cost, wearable, scalable, and suitable for long-term use in hospital and home settings.

Contributions

1. We demonstrate a mobility analysis system, including an IMU-based body sensor network (two sensors embedded in shoes, and one on the waist), a mobile application and a web service for data analysis and visualisation. We designed and developed these sensors to be non-invasive and invisible for day-to-day use, and practical for people with PD.

2. We propose novel and accurate gait analysis algorithms by fusing accelerometer and gyroscope data, combining multiple sensors, and utilising kinematic physical constraints (such as that the shoe-embedded sensor is stationary at middle-stance). We also use a machine learning approach using multi-layer perceptrons to estimate gait parameters. The best algorithm accuracy is found to be a mean absolute error of stride length: 4.0 cm, and step length: 2.6 cm, outperforming existing methods [3, 36, 34].

3. We collect a rich dataset of the walking of 60 participants, including 40 people with PD (in four different stages of the disease). The dataset is diverse, with stride lengths ranging from 29 cm to 159 cm, and step lengths ranging from 12 cm to 82 cm.

4. We validate our MANA system and algorithms on this dataset of 60 participants.

This paper is laid out as follows. The next section contains relevant related work. Then we detail the MANA system, and its design and development. Following that section, we describe the data collection experiment. Then we introduce novel algorithms and show an analysis of the data collected. After the analysis, we describe the accuracy and performance of our system. Finally, in the last section we include future work and directions, as well as conclusions.

RELATED WORK

Gait impairment is a typical symptom of PD [28, 20], and the gait of people with PD has been studied extensively in the medical literature [13, 11]. Parkinsonian gait differs from that of healthy individuals in multiple ways and is therefore used in diagnosis. People with PD may have shuffling steps,

reduced stride length, increased gait instability, reduced arm swing, and freezing of gait [15].

A standard non-invasive PD test is mobility assessment, which aims to quantify movement and give a clinical measure that reflects the degree of mobility impairment. It is used in diagnosis and medical treatment planning in the early phases of the disease. In the latter phases, mobility assessment may also be frequently necessary to monitor disease progression. Mobility assessment includes the quantification of both the lower and upper motor performance. Specifically, for lower motor performance, stride (and step) time and length are the most fundamental and important measures. Additionally, gait variability measures such as traditional statistical quantities (e.g. coefficient of variation) [4], de-trended fluctuation analysis [6], and phase coordination index [31] are extremely useful for clinical evaluation. Early diagnosis of PD has a much lower accuracy (53%) than those who have had it for 5 years or more (88%) [1].

In clinical gait analysis, stride length and stride time are important and fundamental gait quantities which need to be measured. This need has given rise to a large number of highly specialised and expensive systems to measure gait parameters, such as the pressure sensitive walking mat GAITRite[2], the motion-capture camera array Vicon[3], and IMU-based wearable sensors such as APDM Opal[4]. However, these systems have drawbacks and are prohibitively expensive. GAITRite and Vicon are primarily limited to clinical usage as they require dedicated laboratory space and technical expertise, precluding their use in outdoor environments or in the home. GAITRite does not capture the full gait cycle or upper limb movement, as it can only track foot steps on the mat. Vicon systems can capture the entire body movement in 3D space, although they require the user to wear multiple reflective markers on each extremity which is time-consuming, inconvenient and obstructive. These systems are unwieldy, and are not usable outside of a hospital or gait laboratory.

In contrast, IMU-based wearable sensors are portable, convenient, scalable, and do not require a clinical laboratory setting. They can capture whole body motion by wearing sensors on the extremities. APDM provides a proprietary software package (Mobility Lab) to compute gait parameters from the APDM Opal sensors. However, the Opal sensors do not support standard wireless protocols (such as Bluetooth) necessitating the use of additional hardware for data collection. Like other commercial IMU sensor boards (for example Shimmer[5]), APDM does not provide a low level API to perform custom computations on-board the sensor (such as gait analysis or fall detection). Although IMU-based sensors have clear advantages, calculating the basic gait parameters such as stride length is still a complex and challenging research problem.

IMU-based displacement (e.g., stride or step length) estimation algorithms involve the fusion of triaxial accelerometer and

---

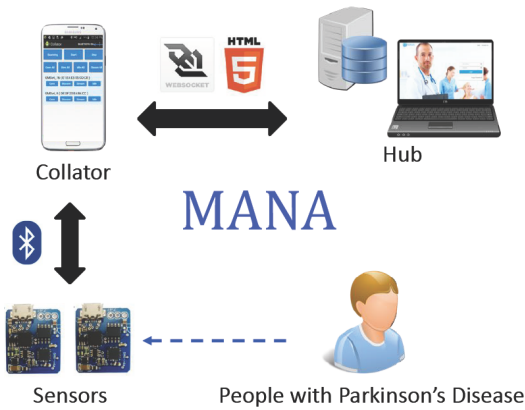[2] http://www.gaitrite.com

[3] http://www.vicon.com

[4] http://www.apdm.com/wearable-sensors

[5] http://www.shimmersensing.com

Figure 1. MANA system overview.

Figure 2. The sensor in its case, and the sensors location in the shoe.

gyroscope data, and they can be generally grouped into three categories: machine learning-based regression methods [37], Kalman filter-based fusion algorithms [16], and double integration of acceleration [5]. Machine learning-based algorithms require a large and comprehensive dataset to train a model that can be generalised to new participants. However, their generalisability needs further validation as most existing studies have a limited number of test participants. Fusion algorithms based on Kalman filters usually require the use of a magnetometer as a reference of orientation, and thus are not suitable for pure IMU-based systems such as ours. Methods based on double integration of acceleration are more straightforward and computationally efficient, although they need to cope with integration drift due to sensor noise and numerical computation errors. A common method to mitigate integration drift is resetting the integration value to zero after each stride [12]. However, such resetting methods may introduce large errors to the stride length estimation if the IMU is not attached to an appropriate and consistent position on the foot [27]. Therefore, many of these methods require improvement in measurement accuracy and usability to be deployable in non-laboratory settings.

MANA SYSTEM

In order to mitigate the drawbacks of the systems described, we designed MANA to be an inexpensive, portable and scalable mobility analysis system built on open standards such as Bluetooth low energy (BLE) and websockets such that it is platform independent and future proof. The most important design considerations were to make the sensors invisible and user friendly, thus reducing the stigma associated with their use. In this section, we describe the components of the MANA system and the design considerations made.

System Description

MANA consists of a series of physical devices, communication protocols, motion analysis algorithms, and software applications. MANA has three main physical components: wearable IMU-based sensors (Sensors), an application running on a mobile device (Collator), and a web application hosted on cloud servers (Hub) (see Figure 1). The general
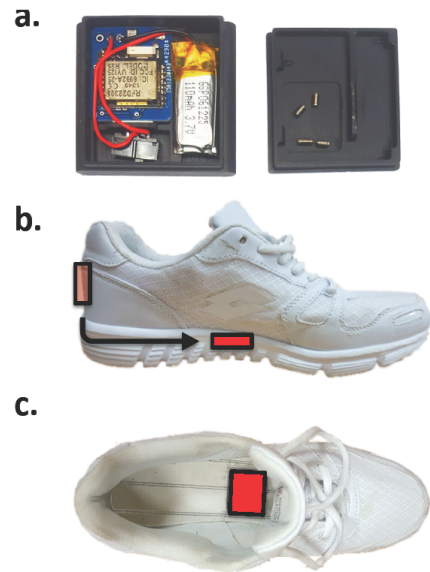
workflow of the system is that a participant can wear the sensors to record motion data, which in turn uploads the data over Bluetooth Low Energy (BLE) to a smartphone via the installed Collator app. The Collator further uploads the data to the server for real-time processing, and the results are sent back to the Collator and also visualised in the web application. This is a closed-loop of real-time data collection, analysis, and feedback to the user. The first component of the system is the sensors, and their specifications and design.

MANA Sensors

The MANA sensor unit (see Figure 2a) is a custom-built printed circuit designed for recording human motion and mobility. The board itself has gone through multiple iterations over the years as can be seen in Figure 3. The earliest versions of the board had minimal computational power, little on board storage, and were relatively bulky. The first Arduino-based units had fairly small memory footprints and required a separate bluetooth module. Though we managed to squeeze one simple gait algorithm onboard the early models [40], it was clear that the RAM available was insufficient for the more sophisticated algorithms we had started to trial. We then moved to the RFduino module which had much more RAM, program space, and an integrated BLE stack. The Simblee is the next generation of the RFduino, and provides the same functionality in a much smaller, single chip footprint. During this development, we also moved from Bluetooth v2.0 to BLE for its reduction in power consumption. Due to the need for a smaller and more feature rich sensor, we significantly improved the board in terms of both hardware specifications and requirements for our users. The latest iteration of the board is a single-sided 20.4mm × 24.1mm PCB, and includes:

- A Simblee IC, which has a 32-bit ARM Cortex M0 at 16MHz, with 24kB of RAM, and 128Kb of program/flash memory.
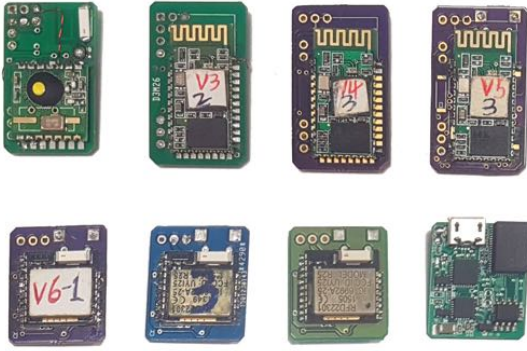
Figure 3. Iteration of sensor hardware over time.

Figure 4. Battery characteristic graph.

- A 6-axis Inertial Measurement Unit (MPU6050). Our unit also supports a 9-axis MPU9150 (with added Magnetometer).

- Support for a real-time location module, the DWM1000. This module can be used for 2-way absolute range measurements, although in this project it is not used.

- Bluetooth and USB connectivity.

- Low power mode for long term and untethered use.

- 256kB of EEPROM, the primary intended use for this is storing processed (step) data, typically a week or two of data.

- Battery, and battery management circuitry for measuring and charging the attached 110mAh LiPo battery.

MANA sensors are programmable and give us full access to the underlying hardware, allowing custom software to be run directly on the sensor. We do not use a magnetometer as they are easily susceptible to magnetic interference which can limit the accuracy of orientation estimates [2]. However, this lack of a magnetometer does not prevent us from estimating stride and step length as is demonstrated in the results section of this paper.

Each sensor draws up to 100mA when charging, and can be recharged in about an hour, by plugging it in to a USB port. A significant amount of effort was spent in ensuring that all components used the least amount of energy, choosing low power components throughout, and only powering components (such as the USB chip) when they are needed. Our sensor software makes use of all such energy saving features. The sensors have been tested to see what sort of battery behaviour they have in long-term use. The ultra low power standby mode (or shelf life) lasts for about two months. Additionally, we tested the battery life in a day-to-day use case of approximately one hour of walking per day and found the devices lasted around two weeks. We also tested the sensors in a test-bed, simulating intensive laboratory use. During our experiment, we attached units to around three test participants every hour, so we used this as a guideline for our test-bed trial. Our test-bed moved the units to simulate walking, and continuously streamed the
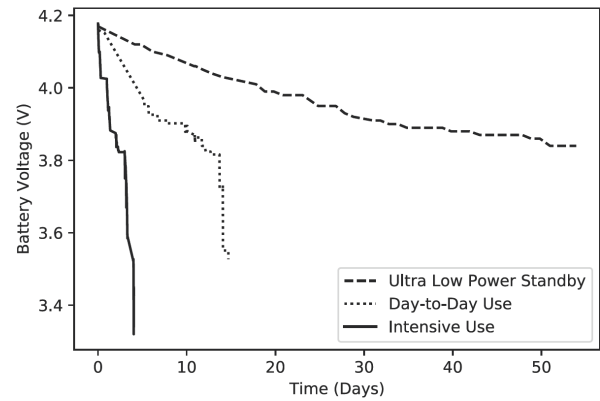
data via Bluetooth, for 10 minutes on, 10 minutes off, 8 hours per day. The units last for 3-4 days between charges. The battery characteristics of all three use cases can be seen in Figure 4.

During data collection, the sensor samples the IMU at 100 Hz, and streams the 3-axis accelerometer and 3-axis gyroscope readings together with the sampling timestamp to the Collator. Transmitting raw sensor data to the Collator in real-time is a challenge for the limited bandwidth of BLE, especially when multiple sensors stream data simultaneously to the same Collator. To maximise the use of the available bandwidth and reduce power consumption, the sensors compress the IMU data before transmission. The compression technique works by sending the differences in adjacent IMU readings (and adjacent timestamps) rather than the raw values, and thus it requires much fewer bytes to represent the data. As per the BLE specification, only 20 bytes can be sent within each time slot, due to the limitation of GATT (Generic Attributes) characteristics. To fully use the BLE bandwidth, multiple IMU samples are combined into a data packet, and multiple data packets are placed into a sending buffer to be sent together. Exactly 20 bytes are taken from the sending buffer and sent in each time slot, so that no bandwidth is wasted. Each data packet contains a sequence number, so that packet loss can be detected. As a result, the compression technique can reduce the data size (and thus required bandwidth) by a factor of two to three during walking data collection. We can stream from five sensors simultaneously to the same Collator without data loss using this compression technique, while data loss occurs frequently if compression is not used.

Since the sensor's hardware clock drifts over time, each sensor will keep a different local time. In our system, every sensor clock is synchronised to the Collator smartphone clock via a simple synchronisation protocol [35]. Specifically, the Collator sends a "get-time" command to the sensor, and the sensor immediately replies with its local time. The Collator also records the time of the smartphone when the command is sent and when the reply is received. This procedure is repeated multiple times before and after data collection. With the resultant timestamp dataset, we can use linear regression to find the best alignment of the sensor time to the smartphone time

Figure 5. Iteration of sensor case over time.

(by calculating an offset and a scale factor of the sensor time). The error bound of the synchronisation is approximately 10 ms, which is accurate enough to align the movement recorded by different sensors (e.g., left and right steps).

In tandem with this sensor development, a custom plastic case has been iterated on to encapsulate the sensor board together with the battery, see Figure 5. Originally, our system used ankle mounted sensors as these provided the best measurements of stride and step length. However, in discussions with clinicians and people with PD we realised that such a design would draw attention to the user of the device, causing embarrassment and discouraging use. We therefore had to re-think our original design and instead moved the sensor underneath the arch of the foot as can be seen in Figure 2 b and c. This simple change of location had many knock-on effects to our system design. For one, the sensor case had to be strong enough such that it was able to withstand the force of footfalls whilst being embedded in the shoes during walking. To meet this requirement we moved from fragile 3D printed cases to a durable plastic machined case. We also based the dimensions of the case on the dimensions of the 6th generation iPod Nano, allowing us to use any of the mounts and cases designed for this product. Furthermore, algorithms designed around the original location had to be redesigned to take into account the physics of the new position of the sensor.

For the needs of our system, our sensors have many benefits over other commercial products. They are inexpensive even before mass production (less than USD $100), they permit us to use wireless transmission, and they are completely programmable. This last feature is critical as in future work we intend to develop more sophisticated onboard algorithms for gait evaluation and detection.

MANA Collator and Hub
The Collator is a mobile application that can run on any smartphone that supports BLE. It collects the data from sensors over BLE and then uploads the data to the Hub. It is currently implemented on the Android platform and has been tested on the most common Android phones (such as the Samsung Galaxy S series). During normal operation, the application runs in the background collecting data from the sensors, and if it has access to the internet it will securely transfer the recorded data to the Hub.

The Hub is a web based application for storing, processing and viewing the data recorded by the MANA sensors. It has an accounts and permission system to only allow a user's data to be seen by those with appropriate authorisation (such as the user himself/herself or the doctor of that user). Additionally, there is an anonymiser system to generalise data for research purposes. The system supports both historical (or archived) data for later analysis and live streaming for real-time data acquisition and processing. The Hub can compute the gait parameters (e.g., stride time and stride length) immediately after each stride, and stream them back to the Collator in real-time. A set of communication protocols are defined and implemented between the Sensor, Collator and the Hub, so that the user can easily control the sensors from both Collator and the Hub.

By connecting the wireless MANA sensors to smartphones and cloud services, MANA becomes an all-in-one system with access to both real-time motion tracking and almost unlimited computing power, allowing sophisticated temporal and spatial gait analysis to be performed. MANA was designed with people with PD in mind, specifically to reduce the stigma of using any assistive technology. With this system built, we ran a clinical data collection experiment to validate our system and algorithms.

DATA COLLECTION EXPERIMENT
To test our new system, algorithms, technology and applications, we designed and performed a clinical experiment at Huashan Hospital, Fudan University in Shanghai, China.

Experiment Protocol
The intention of this experiment was to test our system across a large and diverse set of participants with varying degrees of gait disability. We recruited forty people with PD, ten participants for each severity group and ten people with rapid eye movement sleep behaviour disorder, a prodromal condition for PD. Additionally, ten age and sex matched healthy participants were recruited from the public. In total there were sixty participants. Participants could be included if they met the following criteria:

- Between 50-75 years old.

- Capable of reading, understanding, and signing the informed consent (no cognitive impairment).

- No serious diseases or conditions which would effect their ability to perform the tasks required.

- No gait disabilities or symptoms caused by other disorders which could affect analysis.

All testing procedures were approved by the Institutional Review Board (IRB) at Huashan Hospital, and all participants signed consent forms. All participants were recruited from the
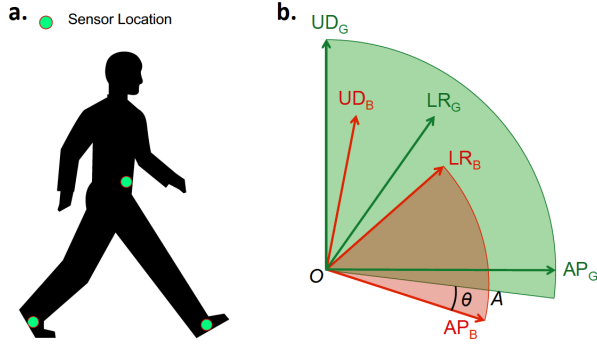
Figure 6. Sensor locations on the body, and the transformation between sensor body and global reference frames.

Figure 7. Example of IMU data.

Figure 8. Annotated gait segment.

Parkinson's Database Study of Huashan Hospital. Participants were required to be in a medication deplete state to fully show their symptoms during the trial.

Participants were evaluated by neurologists on the day of the test to give an evaluation of their disease stage. Data on severity of gait disability, as well as other important data such as height, weight, age and so forth were collected on each participant. All of the experiment was filmed to serve as ground truth and also for blind testers to evaluate the status of each participant. Each participant was equipped with five sensors, though here we only use the following three, two embedded in the shoes, and one on the waist (see Figure 6a), which recorded accelerometer and gyroscope data at 100 Hz. We tested our system against ground truth measurements of stride length and step length. We obtained our ground truth measurement for stride length by using a computer vision based system similar to that in [42].

Test Procedure
The test procedure involved walking on an eight metre walking track. Participants were required to walk unassisted approximately 8-10 times around this walking track continuously to give a minimum of around 30 strides of each foot. The walking track has two turns, one at the beginning and one at the end. Participants could stop at any time if they were unable to continue. In the next section, we will discuss the algorithms used to calculate gait parameters from this recorded accelerometer and gyroscope data.

ALGORITHMS AND ANALYSIS
One of the key functionalities of MANA is gait analysis. The first step of analysis involves segmenting each stride from the IMU data, and identifying each stage in a gait cycle. After that we can calculate the temporal gait parameters (e.g., step and stride time) and spatial gait parameters (e.g., step and stride length). This section describes the IMU data processing pipeline for temporal and then spatial gait analysis.

Data Preprocessing
Before the accelerometer and gyroscope data can be analysed by our algorithms it must first be calibrated, then converted to a consistent reference frame. After that, the data is separated into straight line walking segments, and into non-walking segments.
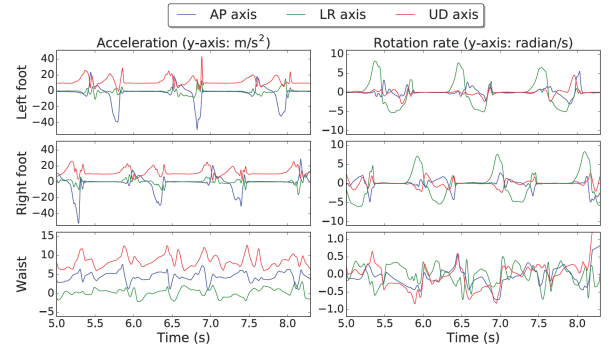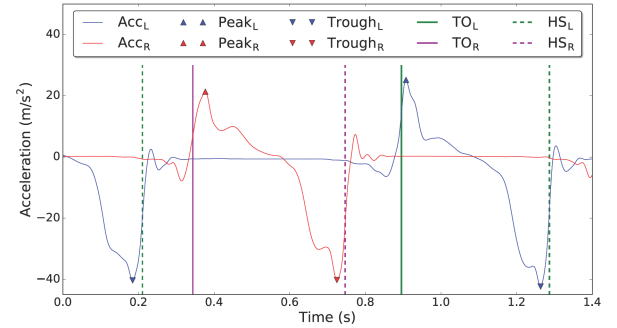
Accelerometer and Gyroscope Calibration
Each axis i of an accelerometer or gyroscope has a bias b_i and scale factor f_i, which are required to adjust the raw sensor measurement V_i^{raw} to the calibrated value V_i^{calib} for further processing:

$$V_i^{calib} = f_i(V_i^{raw} - b_i).$$

For the inertial sensors such as the ones used in our system, the sensor parameters b_i and f_i are different for different sensors, and also vary under different temperatures. Thus we conduct a one-time lab calibration to obtain the baseline parameters for each sensor, and use these parameters to adjust the raw sensor measurements. Since in each data collection session, the actual sensor parameters may vary slightly, we introduce b_i and f_i as variables in one of our sensor models and fine-tune them in each session.

To perform this one-time lab calibration of each axis of the accelerometer and gyroscope, we built a calibration platform which can be programmed to rotate in two degrees of freedom. Then we affix the sensor board on the platform, and use the sensor readings when the platform is stationary or rotating to calibrate each axis of the accelerometer and gyroscope [40].

IMU Coordinate System
The next step is to change the IMU coordinate system to one that is more intuitive and straightforward. Each shoe sensor

is embedded in the shoe such that the three IMU axes are approximately parallel with the forward, leftward and upward directions of the participant, respectively. The sensor body frame constructed by the three IMU axes is denoted by $\{\mathscr{B}\}$. For simplicity and convenience, from the participant's perspective, we define the three IMU axes as anterior-posterior (AP) axis (anterior as positive direction), left-right (LR) axis (leftward as positive direction), and up-down (UD) axis (upward as positive direction), which are denoted by $\vec{AP}_B$, $\vec{LR}_B$ and $\vec{UD}_B$, respectively (Figure 6b). These three axes form a right-handed Cartesian coordinate system. Thus the 3-axis acceleration can be denoted by a_{AP}, a_{LR} and a_{UD}, respectively. Similarly, the 3-axis rotation rates measured by the gyroscope are denoted by ω_{AP}, ω_{LR} and ω_{UD}, respectively. Example accelerometer and gyroscope waveforms are shown in Figure 7.

Since the time interval between successive IMU samples varies slightly (even though the IMU is configured to sample at a constant rate), the raw IMU data is usually interpolated and resampled at a higher fixed frequency [14, 21]. In our study, all IMU data was cubic-spline interpolated and resampled at 1000 Hz, and then low-pass filtered at a cut-off frequency of 10 Hz, as is common in most studies [43, 44].

Straight Line Walking Segmentation
We focus only on the analysis of gait data during straight-line walking. Therefore, a program was developed to separate straight-line walking segments from non-walking segments such as stationary or turning segments. This separation was achieved primarily based on manually selected thresholds of the acceleration amplitude (to remove non-walking segments) and rotation rate (to identify turning). Since the patterns of different walking segments are relatively prominent and clear in the walking dataset collected in this study, this straight-line walking segmentation program achieved close to 100% accuracy.

Gait Cycle Analysis
Temporal gait analysis involves the segmentation of each individual stride (known as a gait cycle) from the IMU data. Figure 9 illustrates different phases in a full gait cycle, such as swing/stance phases and single/double support phases. These gait phases are separated by Toe-Off (TO) and Heel-Strike (HS) events. The step time is the duration between two successive HS of the two feet, while the stride time is between two successive HS of the same foot. The stance phase of one foot is from its HS to its TO. The swing phase of one foot is from its TO to its HS, which corresponds to the single-support phase of the other foot. The double-support phase is between the HS of one foot and the TO of the other foot. The duration of each phase in the gait cycle can be directly obtained from the TO and HS times of both feet.

As shown in Figure 8, each TO and HS event in a stride causes a predominant peak and trough in the a_{AP} waveform. The peak and trough points can be located using a simple peak detection algorithm. To find stable and reliable correspondence points of the TO and HS events in the a_{AP} waveform, we use the sharpest rising point (i.e., with the largest difference between this point and its preceding point) in the rising edge preceding the peak point as the correspondence point of a TO event, and use the sharpest rising point in the rising edge after the trough point as the correspondence point of a HS event.

Whilst a single sensor attached to the waist at the navel position can also be used by itself to detect steps and strides and even identify left vs. right steps [41, 9], it is usually not as straightforward and accurate as detection based on two foot-attached sensors. This is an advantage of our sensor system which allows the whole gait cycle to be clearly defined. This complete gait cycle analysis cannot be achieved by a single sensor on one foot or on the waist. For example, one sensor can not detect strides of the opposite foot. Moreover, double-support time and single-support time of the opposite foot can not be inferred from one sensor.

After gait cycle analysis, statistics of an entire walking session can be calculated, such as step count, cadence (steps per minute), variation of step time, and swing/stance time ratio. The comparison of these parameters between two feet (e.g., left/right step time ratio) can also be performed. To clinicians, these results of the temporal analysis provide insights into the gait dynamics and walking style of the participant and subsequently to the participant's health condition. For instance, some people with PD are more impaired on one side of the body than the other, and as such they tend to have imbalanced gait, which is usually reflected as a large difference between some or all gait parameters of two feet.

Stride Length Calculation
Now that the gait cycle of each stride is clearly defined, we can calculate stride length, which is an important and fundamental spatial gait parameter. The position of the IMU affects the accuracy of stride length estimation [27]. Due to our users requirements we embedded the sensor in the bottom of the shoe which enforced several kinematic constraints that can be used in our algorithms. The following subsections describe two stride length algorithms based on double integration and kinematic constraints, which use the data from a single shoe-embedded sensor.

The stride length is the distance between two stance positions of the same foot. As the foot sensor is embedded in the shoe, the sensor stays stationary during the stance phase of the gait cycle, and therefore all axes of IMU data do not vary much. This is clearly shown in Figure 8 as the segment of the waveform which is flat and approximately zero for both accelerometer and gyroscope. Thus, we define the middle time point of the stance phase as the "zero point", because at "zero point" the gravity-removed acceleration, velocity, and rotation rate of the IMU can all be assumed to be zero. This definition is consistent with the "zero velocity assumption" [12] and the Zero Velocity Update method (ZUPT) at mid-stance that are widely adopted by many studies for foot-mounted IMU analysis. Unlike our study, the IMU in those studies is attached to the back of the heel or the ankle position, causing the IMU to slowly rotate during stance. In general, the higher the sensor is attached on the foot, the faster the sensor rotates at stance. Research has shown that multiple significant modelling errors are related to the ZUPT methods [27]. By contrast, our shoe-embedded sensors have almost constant readings at "zero
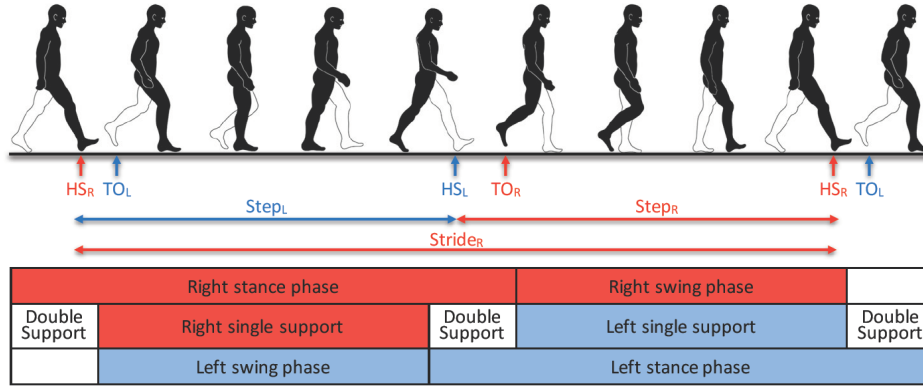
Figure 9. The gait cycle.

point", which results in smaller errors and justifies the use of the "zero velocity assumption".

Transformation Between Coordinate Systems

As stride length is measured in the global reference frame (denoted by $\{\mathscr{G}\}$), we must transform the IMU acceleration from the sensor body frame to the global frame. Assuming straight-line walking on level ground, a global coordinate system $\{\mathscr{G}\}$ can be established with its AP axis ($\overrightarrow{AP}_G$) pointing forwards along the walking line, its LR axis ($\overrightarrow{LR}_G$) pointing leftwards of the participant, and UD axis ($\overrightarrow{UD}_G$) pointing upwards (parallel with gravity direction). During straight-line walking, the global coordinate system $\{\mathscr{G}\}$ is fixed, while the sensor body frame $\{\mathscr{B}\}$ rotates along with the shoe. The acceleration recorded by the IMU is represented in $\{\mathscr{B}\}$, while the spatial gait parameters such as stride length are represented in $\{\mathscr{G}\}$. Thus the first step is to transform the acceleration into $\{\mathscr{G}\}$. Let R be the transformation matrix from $\{\mathscr{B}\}$ to $\{\mathscr{G}\}$, thus the acceleration vector $a^B = [a_{AP}, a_{LR}, a_{UD}]^T$ measured by IMU in $\{\mathscr{B}\}$ can be transformed to acceleration in $\{\mathscr{G}\}$ as $a^G = Ra^B$. Double-integrating a^G gives the distances traveled in the global frame, such as stride length.

During walking, R changes in time, and is denoted by $R(t)$ at time t. Time t starts from 0 (at the beginning of the stride) and ends at T (at the end of the stride). First, we need to determine $R(0)$, i.e., the rotation of the shoe at the start of a stride.

Since the IMU is assumed to be stationary in the beginning of a stride, the acceleration measured should be purely acceleration due to gravity. We introduce a parameter θ as the angle between the direction of movement in the global frame and the AP axis, as shown in Figure 6b. Usually θ is relatively small as the IMU is embedded in the shoe such that they are almost co-directional. The parameter θ will be determined differently later in the two algorithms described in the next subsections.

After $R(0)$ is obtained, and given the IMU rotation rate $\omega(t) = [\omega_{AP}(t), \omega_{LR}(t), \omega_{UD}(t)]$ measured by the gyroscope at time t, $R(t)$ can be updated iteratively by

$$R(t+dt) = R(t) \begin{bmatrix} 1 & -\omega_{UD}(t)dt & \omega_{LR}(t)dt \\ \omega_{UD}(t)dt & 1 & -\omega_{AP}(t)dt \\ -\omega_{LR}(t)dt & \omega_{AP}(t)dt & 1 \end{bmatrix},$$

where dt is a small time interval between two IMU samples [17, 32].

Note that this equation integrates $\omega(t)$ over time, which may cause an accumulated estimation error of $R(t)$ due to the noise in $\omega(t)$ and the errors of numerical integration. This is the main source of error in this stride length estimation approach and the next subsections will describe the general idea of different methods to compensate for it, a more in-depth overview can be found in [39].

Reset-based Stride Length Algorithm (SL-Reset)

The key idea of the Reset-based Stride Length Algorithm is to linearly reset the gravity-removed acceleration and velocity to zero at the end of each stride, which is a zero point. As mentioned before, $R(t)$ usually drifts over time, which can cause increasing estimation errors. At the stride ending time $t = T$, the acceleration in the global frame may be far from zero, even though based on the zero point assumption, it should be close to zero. To mitigate this drift problem, the following linear resetting function $h_0(\cdot)$ is applied to the acceleration to force it to be zero at $t = T$:

$$h_0(x(t)) = x(t) - \frac{t}{T}x(T),$$

where $x(t)$ is a time series with t between 0 and T.

Optimisation-based Stride Length Algorithm (SL-Opt)

The Optimisation-based Stride Length Algorithm utilises a sensor fusion model with parameters and then optimises these parameters based on kinematic constraints. As mentioned, the sensor bias and scale factor may change under different environments, or even after each switch-on. To account for these variable sensor properties, we first process the sensor data using the following models. The acceleration model used in this method is given by

$$a_i = (1 + f_i^{Acc})(\tilde{a}_i - b_i^{Acc}),$$

where i is one of the AP, LR or UD axes, $\tilde{a}_i$ is the IMU-measured acceleration after preprocessing, b_i^{Acc} is the bias, and f_i^{Acc} is the adjustment of the scale factor. Similarly the model for rotation rate ω_i is

$$\omega_i = (1 + f_i^{Gyro})(\tilde{\omega}_i - b_i^{Gyro}).$$

The 12 model parameters $\Omega = \{b_i^{Acc}, f_i^{Acc}, b_i^{Gyro}, f_i^{Gyro}\}_i$ will be estimated later using least-squares optimisation (such as using the Levenberg–Marquardt algorithm [25]). Finally, after the model parameters Ω and θ are determined, the stride length is calculated.

Linear Correction of SL-Reset and SL-Opt
In the previous two approaches, we found that the derived stride lengths had a mean error of approximately 2-4 cm, instead of zero (see the results in Table 1). The underestimation of stride length is likely caused by several reasons. For example, since the IMU data is low-pass filtered in the preprocessing step in order to remove noise, the amplitude of the resultant data is inevitably reduced to some extent, which leads to a reduction in stride length estimation. Another source of this underestimation is that in reality the velocity at zero points may be slightly larger than zero for some strides, thus resetting the velocity to zero can cause an underestimated stride length.

In order to compensate for this underestimation, we fit a model to map the initial stride length estimation (L') to the ground-truth stride length (L). Since this is a simple mapping between two scalar variables, we used a regression model. Specifically, different degrees of polynomial regression models were trained and evaluated, and we selected simple linear regression (i.e., $L = \alpha L' + \beta$) for its accuracy and parsimony, where the coefficients α and β are determined using least squares fitting.

Machine Learning Regression for Stride Length (SL-ML)
Another approach is to use machine learning methods to estimate stride length. For each stride, we extracted features from the IMU waveforms of both foot sensors. For the three acceleration waveforms (and similarly for the three rotation rate waveforms), the first and second integral of each waveform as well as the energy waveform (i.e., the Euclidean norm) are used. Approximately 5000 features are extracted from each waveform, and are similar to those in existing studies [41], such as the min, max, mean and standard deviation of each waveform.

We used Multi-layer Perceptrons (MLP) to build our regression models in this study, due to their flexible configuration and modelling capability, as well as their wide application (with validated performance) in gait analysis (e.g., [37, 41]). We use the `scikit-learn` library [30] to train the regression model. Our process involves

1. Feature standardisation by centering and scaling the features to zero mean and unit variance.

2. Feature dimensionality reduction using Principal Component Analysis (PCA).

3. Training and evaluation of the regression model.

We split the data into 80% for training and validation sets, with the remaining 20% as a test set. The sets are split such that the ratio of steps of each participant is the same in all sets. We performed five-fold cross-validation using the training and validation sets to tune the MLP hyper-parameters. The final

Table 1. Measurement errors of our three stride length estimation algorithms and comparison to other studies

Algorithm	Error: cm (% error)	
	Mean	MAE
SL-Reset Initial	-3.78 (-3.09)	6.9 (5.71)
SL-Reset Corrected	0.03 (0.02)	6.72 (5.68)
SL-Opt Initial	-2.16 (1.8)	5.78 (4.8)
SL-Opt Corrected	0.02 (0.02)	5.72 (4.71)
SL-ML	-0.63 (0.27)	**4.04 (4.24)**
Bamberg et al. [3]	-	8.50 (-)
Sijobert et al. [36]	-	9.00 (5.60)

model performance is evaluated on the test set. Our best hyper-parameters were found to be 40-100 PCA components, and a single hidden layer of size 800.

Machine Learning Regression for Step Length (StepL-ML)
Step lengths (as distinct from stride lengths) are another important spatial gait parameter for clinicians to evaluate gait [23, 18]. As described in the previous subsections stride length can be calculated analytically based on the zero point constraints using a shoe-embedded sensor. However, it is not as straight-forward to calculate the step length between alternating feet purely based on two shoe-embedded sensors, since one sensor can only measure the movement of the foot that it is mounted on and it is difficult to align the two sensor positions spatially.

In the MANA system, the waist-mounted sensor can be used to measure step length since the waist sensor captures the movement of both feet. The previous stride length methods rely on the assumption that the IMU is stationary at the middle of stance and thus it is not suitable for step length calculation using the waist sensor, because the waist sensor keeps moving forward even during the foot stance phase.

To calculate step length based on the waist sensor, machine learning-based regression methods were used, as have been adopted by many studies for IMU-based displacement measures, including step and stride length [41]. We repeated the same procedure using an MLP as in the previous subsection, but this time using the waist sensor data in addition to the foot sensor data. Our best hyper-parameters were found to be 100 PCA components, and a single hidden layer of size 700.

RESULTS
A stride length dataset of 5141 strides from both feet was combined across 60 participants, with a minimum of 30 strides for each participant. Since the participants vary from healthy participants to participants with severe PD, the stride length dataset has a large range from 29 cm to 159 cm. The mean and standard deviation of the stride lengths are 102 cm and 24 cm, respectively.

Three stride length algorithms (SL-Reset, SL-Opt, and SL-ML) were tested on this dataset and compared to ground truth measurements. Different metrics have been used in the literature to quantify such measurement errors, and here we report the mean error, and mean absolute error (MAE) measured in cm for each algorithm, as shown in Table 1. Furthermore, since the stride length varies across a large range, we also

Table 2. Measurement error of step length estimation algorithm and comparison to other studies

Algorithm	Error: cm (% error)	
	Mean	MAE
StepL-ML	-0.01 (0.76)	**2.63 (5.86)**
Sayeed et al. [34]	-	3.30 (-)
Zhu et al. [41]	-	RMSE: 3.22 (6.95)

Table 3. Breakdown of measurement error of stride and step length estimation algorithms by severity group

Algorithm	Error MAE: cm (% error)		
	Healthy	Mild	Severe
SL-ML	4.08 (3.24)	3.80 (3.62)	4.23 (5.45)
StepL-ML	2.66 (4.32)	2.14 (4.04)	3.05 (8.40)

calculated the normalised percentage error, which is the estimation error divided by the ground-truth stride length and multiplied by 100. Each row in the table represents a different condition of the algorithm, where "Initial" means the original estimation of stride length without applying the linear regression method, and "Corrected" means that linear regression was applied.

As can be seen in Table 1, these errors of the proposed algorithms are dramatically smaller than other IMU-based studies that are tested on people with PD. It is worth noting that our study involves a large group of participants with a wide range of gait styles and stride lengths. By applying linear regression, the mean error of all algorithms is reduced to almost zero. A mean error of about zero indicates an accurate algorithm for estimating the total walking distance (such as in pedestrian tracking), and outperforms existing studies. However, SL-ML is the best performing and has the smallest mean absolute error of approximately 4.0 cm (or 4.3%).

A step length dataset of 4857 steps was combined across the 60 participants. The size of the step length dataset is slightly smaller than the stride length dataset because each step requires the existence of two strides of both feet. The step length dataset ranges from 12 cm to 82 cm, with a mean of 51 cm and standard deviation 12 cm. The results of our step length algorithm accuracy can be seen in Table 2. As can be seen in the same table, by incorporating the information from the foot sensor and waist sensor, StepL-ML has an accuracy that is comparable to (or better than) other studies of the same type. Whilst a direct comparison can not be made with Zhu et al. [41], the RMSE error is of the same order as our study.

We also looked at the performance of our system as a function of PD severity. We split our 60 subjects into three groups of increasing severity, those without PD, those with PD in stages 1 and 2, and finally those with PD in stages 3 and 4. We then evaluated our best performing stride length and step length algorithms on these groups. As can be seen in Table 3, the accuracy of the system is slightly lower in the more severe cases. This is expected as in late stages of the disease, walking patterns can become more erratic. Despite this, it still outperforms the other studies in Table 1 and 2.

In summary, by measuring stride and step length for both feet, MANA can provide comprehensive insights into spatial gait dynamics, as well as the statistics (e.g., variation) and comparison between two feet, which is a fundamental part of gait and mobility analysis.

FUTURE WORK AND CONCLUSIONS

In this paper we demonstrated an all-in-one system for mobility analysis, including a body sensor network (two sensors embedded in the shoes, and one on the waist) and a data analysis and visualisation backend. We introduced novel and accurate gait analysis algorithms by fusing accelerometer and gyroscope data and using imposed kinematic constraints. We also use machine learning techniques to calculate stride and step metrics accurately. Additionally, we performed a clinical trial with 60 participants, 40 people with PD, 10 people with rapid eye movement sleep behaviour disorder, and 10 healthy people to validate our system and algorithms.

By taking into account our users' requirements, and putting the user center in our development, we were able to find new and innovative methods to estimate gait metrics. For example, embedding the sensor in the shoe enabled the development of novel algorithms for gait length estimation. This is an important differentiating characteristic of our system in contrast to most commercial systems which use ankle mounted sensors. This new location is shown to be an advantage for some stride length estimation algorithms (specifically for justifying zero point assumptions). Furthermore, the unobtrusiveness of the sensor location and the long battery life makes long term monitoring using MANA a strong possibility.

The flexibility, portability, and scalability of MANA enables a wide range of applications and use cases with high social impact. Firstly, MANA provides people with PD with affordable access to gait analysis technology normally only available at large hospitals. Systems such as the GAITRite cost many tens of thousands of dollars, whereas each of our sensors cost less than USD $100. MANA can be used at home as it is a convenient and invisible wearable system designed to limit the stigma associated with assistive technologies. It makes it possible for someone to track their motor performance over a much longer time period, providing more accurate and fine-grain information. Our system also allows for up to five sensors recording data at one time, meaning sensors could be placed on other extremities to record other human motion.

MANA is not only restricted to monitoring people with PD; it can also be used for evaluation of those with mobility impairment in general. MANA lays out the technical foundation for higher level applications to be developed and deployed. For example, MANA could detect other parkinsonian symptoms such as freezing of gait and perhaps provide audio or visual cues to help a user resume walking. In conclusion, MANA represents a promising platform for accessible and affordable clinical mobility analysis with a wide range of potential applications.

ACKNOWLEDGMENTS

REFERENCES

1. Charles H Adler, Thomas G Beach, Joseph G Hentz, Holly A Shill, John N Caviness, Erika Driver-Dunckley, Marwan N Sabbagh, Lucia I Sue, Sandra A Jacobson, Christine M Belden, and others. 2014. Low clinical diagnostic accuracy of early vs advanced Parkinson disease Clinicopathologic study. *Neurology* 83, 5 (2014), 406–412.

2. Eric R Bachmann, Xiaoping Yun, and Anne Brumfield. 2007. Limitations of attitude estimation algorithms for inertial/magnetic sensor modules. *Robotics & Automation Magazine, IEEE* 14, 3 (2007), 76–87.

3. Stacy J Morris Bamberg, Ari Y Benbasat, Donna Moxley Scarborough, David E Krebs, and Joseph A Paradiso. 2008. Gait analysis using a shoe-integrated wireless sensor system. *Information Technology in Biomedicine, IEEE Transactions on* 12, 4 (2008), 413–423.

4. O. Blin, A. M. Ferrandez, and G. Serratrice. 1990. Quantitative analysis of gait in Parkinson patients: increased variability of stride length. *J. Neurol. Sci.* 98, 1 (Aug 1990), 91–97.

5. F Bugané, MG Benedetti, and others. 2012. Estimation of spatial-temporal gait parameters in level walking based on a single accelerometer. *Comp Meth and Prog in Biomed* 108, 1 (2012), 129–137.

6. S. Damouras, M. D. Chang, E. Sejdi, and T. Chau. 2010. An empirical examination of detrended fluctuation analysis for gait data. *Gait Posture* 31, 3 (Mar 2010), 336–340.

7. Katherine Deibel. 2013. A Convenient Heuristic Model for Understanding Assistive Technology Adoption. In *Proceedings of the 15th International ACM SIGACCESS Conference on Computers and Accessibility (ASSETS '13)*. ACM, New York, NY, USA, Article 32, 2 pages.

8. Miguel Fernandez del Olmo and Javier Cudeiro. 2005. Temporal variability of gait in Parkinson disease: Effects of a rehabilitation programme based on rhythmic sound cues. *Parkinsonism & Related Disorders* 11, 1 (2005), 25–33.

9. Robert J. Ellis, Yee Sien Ng, Shenggao Zhu, Dawn M. Tan, Boyd Anderson, Gottfried Schlaug, and Ye Wang. 2015. A Validated Smartphone-Based Assessment of Gait and Gait Variability in Parkinson's Disease. *PLoS ONE* 10, 10 (10 2015), 1–22.

10. Heather A. Faucett, Kate E. Ringland, Amanda L. L. Cullen, and Gillian R. Hayes. 2017. (In)Visibility in Disability and Assistive Technology. *ACM Trans. Access. Comput.* 10, 4, Article 14 (Oct. 2017), 17 pages.

11. B. Galna, S. Lord, and L. Rochester. 2013. Is gait variability reliable in older adults and Parkinson's disease? Towards an optimal testing protocol. *Gait Posture* 37, 4 (Apr 2013), 580–585.

12. Jeffrey M Hausdorff. 2007. Gait dynamics, fractals and falls: finding meaning in the stride-to-stride fluctuations of human walking. *Human Movement Science* 26, 4 (2007), 555–589.

13. Jeffrey M Hausdorff, Zvi Ladin, and Jeanne Y Wei. 1995. Footswitch system for measurement of the temporal parameters of gait. *J Biomechanics* 28, 3 (1995), 347–351.

14. Tuck-Voon How, Justin Chee, Eric Wan, and Alex Mihailidis. 2013. MyWalk: a mobile app for gait asymmetry rehabilitation in the community. In *Proc. PervasiveHealth*. ICST, 73–76.

15. J. Jankovic. 2008. Parkinson's disease: clinical features and diagnosis. *J. Neurol. Neurosurg. Psychiatry* 79, 4 (Apr 2008), 368–376.

16. Antonio Ramón Jiménez, Fernando Seco, José Carlos Prieto, and J Guevara. 2010. Indoor pedestrian navigation using an INS/EKF framework for yaw drift reduction and a foot-mounted IMU. In *2010 7th Workshop on Positioning Navigation and Communication (WPNC)*. IEEE, 135–143.

17. Robert Mahony, Tarek Hamel, and Jean-Michel Pflimlin. 2008. Nonlinear complementary filters on the special orthogonal group. *IEEE Trans. Automat. Control* 53, 5 (2008), 1203–1218.

18. M. K. Mak. 2013. Reduced step length, not step length variability is central to gait hypokinesia in people with Parkinson's disease. *Clin Neurol Neurosurg* 115, 5 (May 2013), 587–590.

19. Tara McCurdie, Svetlena Taneva, Mark Casselman, Melanie Yeung, Cassie McDaniel, Wayne Ho, and Joseph Cafazzo. 2012. mHealth consumer apps: the case for user-centered design. *Biomedical instrumentation & technology* 46, s2 (2012), 49–56.

20. Marie E McNeely, Ryan P Duncan, and Gammon M Earhart. 2012. Medication improves balance and complex gait performance in Parkinson disease. *Gait & Posture* 36, 1 (2012), 144–148.

21. Sabato Mellone, Carlo Tacconi, and Lorenzo Chiari. 2012. Validity of a Smartphone-based instrumented Timed Up and Go. *Gait & Posture* 36, 1 (2012), 163–165.

22. Hylton B Menz, Mark D Latt, and others. 2004. Reliability of the GAITRite walkway system for the quantification of temporo-spatial parameters of gait in young and older people. *Gait & Posture* 20, 1 (2004), 20–25.

23. R. Moe-Nilssen, M. K. Aaslund, C. Hodt-Billington, and J. L. Helbostad. 2010. Gait variability measures may represent different constructs. *Gait Posture* 32, 1 (May 2010), 98–101.

24. Thomas B Moeslund, Adrian Hilton, and Volker Krüger. 2006. A survey of advances in vision-based human motion capture and analysis. *Computer Vision and Image Understanding* 104, 2 (2006), 90–126.

25. Jorge J Moré. 1978. The Levenberg-Marquardt algorithm: implementation and theory. In *Numerical analysis*. Springer, 105–116.

26. United Nations. 2015. *World Population Ageing 2015*. United Nations, Department of Economic and Social Affairs, Population Division.

27. John-Olof Nilsson, Isaac Skog, and Peter Händel. 2012. A note on the limitations of ZUPTs and the implications on sensor error modeling. In *2012 International Conference on Indoor Positioning and Indoor Navigation (IPIN), 13-15th November 2012*. 163–165.

28. C Warren Olanow, Yves Agid, and others. 2004. Levodopa in the treatment of Parkinson's disease: current controversies. *Movement Disorders* 19, 9 (2004), 997–1005.

29. Phil Parette and Marcia Scherer. 2004. Assistive technology use and stigma. *Education and Training in Developmental Disabilities* (2004), 217–226.

30. F. Pedregosa, G. Varoquaux, A. Gramfort, V. Michel, B. Thirion, O. Grisel, M. Blondel, P. Prettenhofer, R. Weiss, V. Dubourg, J. Vanderplas, A. Passos, D. Cournapeau, M. Brucher, M. Perrot, and E. Duchesnay. 2011. Scikit-learn: Machine Learning in Python. *Journal of Machine Learning Research* 12 (2011), 2825–2830.

31. M. Plotnik, N. Giladi, and J. M. Hausdorff. 2007. A new measure for quantifying the bilateral coordination of human gait: effects of aging and Parkinson's disease. *Exp Brain Res* 181, 4 (Aug 2007), 561–570.

32. William Premerlani and Paul Bizard. 2009. *Direction Cosine Matrix IMU: Theory*. Technical report.

33. Halley P. Profita, Abigale Stangl, Laura Matuszewska, Sigrunn Sky, and Shaun K. Kane. 2016. Nothing to Hide: Aesthetic Customization of Hearing Aids and Cochlear Implants in an Online Community. In *Proceedings of the 18th International ACM SIGACCESS Conference on Computers and Accessibility (ASSETS '16)*. ACM, New York, NY, USA, 219–227.

34. Taufique Sayeed, Albert Samà, Andreu Català, Alejandro Rodríguez-Molinero, and Joan Cabestany. 2015. Adapted step length estimators for patients with Parkinson's disease using a lateral belt worn accelerometer. *Technology & Health Care* 23, 2 (2015), 179 – 194.

35. Mihail L Sichitiu and Chanchai Veerarittiphan. 2003. Simple, accurate time synchronization for wireless sensor networks. In *Wireless Communications and Networking, 2003. WCNC 2003. 2003 IEEE*, Vol. 2. IEEE, 1266–1273.

36. Benoît Sijobert, Mourad Benoussaad, Jennifer Denys, Roger Pissard-Gibollet, Christian Geny, and Christine Azevedo Coste. 2015. Implementation and Validation of a Stride Length Estimation Algorithm, Using a Single Basic Inertial Sensor on Healthy Subjects and Patients Suffering from Parkinson's Disease. *ElectronicHealthcare* (2015), 704–714.

37. Yoonseon Song, Seungchul Shin, Seunghwan Kim, Doheon Lee, and Kwang Hyung Lee. 2007. Speed estimation from a tri-axial accelerometer using neural networks. In *Engineering in Medicine and Biology Society, 2007. EMBS 2007. 29th Annual International Conference of the IEEE*. IEEE, 3224–3227.

38. Chris Vincent and Ann Blandford. 2011. Designing for safety and usability: User-centered techniques in medical device design practice. In *Proceedings of the Human Factors and Ergonomics Society Annual Meeting*, Vol. 55. SAGE Publications Sage CA: Los Angeles, CA, 793–797.

39. Shenggao Zhu. 2017. *Inertia Sensor-based Mobility Analysis for Parkinson's Disease*. Ph.D. Dissertation.

40. Shenggao Zhu, Hugh Anderson, and Ye Wang. 2012. A real-time on-chip algorithm for IMU-Based gait measurement. In *Advances in Multimedia Information Processing–PCM 2012*. Springer, 93–104.

41. Shenggao Zhu, Robert J Ellis, Gottfried Schlaug, Yee Sien Ng, and Ye Wang. 2014. Validating an iOS-based Rhythmic Auditory Cueing Evaluation (iRACE) for Parkinson's Disease. In *Proceedings of the ACM International Conference on Multimedia*. ACM, 487–496.

42. Wei Zhu, Boyd Anderson, Shenggao Zhu, and Ye Wang. 2016. A Computer Vision-Based System for Stride Length Estimation using a Mobile Phone Camera. In *Proceedings of the 18th International ACM SIGACCESS Conference on Computers and Accessibility*. ACM, 121–130.

43. Wiebren Zijlstra. 2004. Assessment of spatio-temporal parameters during unconstrained walking. *European J Applied Physiology* 92, 1-2 (2004), 39–44.

44. Wiebren Zijlstra and At L Hof. 2003. Assessment of spatio-temporal gait parameters from trunk accelerations during human walking. *Gait & Posture* 18, 2 (2003), 1–10.